

Enhanced mobility of organic thin film transistors by water absorption of collagen hydrolysate gate dielectric

Chao-Ying Hsieh, Jenn-Chang Hwang, Ting-Hao Chang, Jiun-Yi Li, Shih-Han Chen et al.

Citation: *Appl. Phys. Lett.* **103**, 023303 (2013); doi: 10.1063/1.4813075

View online: <http://dx.doi.org/10.1063/1.4813075>

View Table of Contents: <http://apl.aip.org/resource/1/APPLAB/v103/i2>

Published by the [AIP Publishing LLC](#).

Additional information on *Appl. Phys. Lett.*

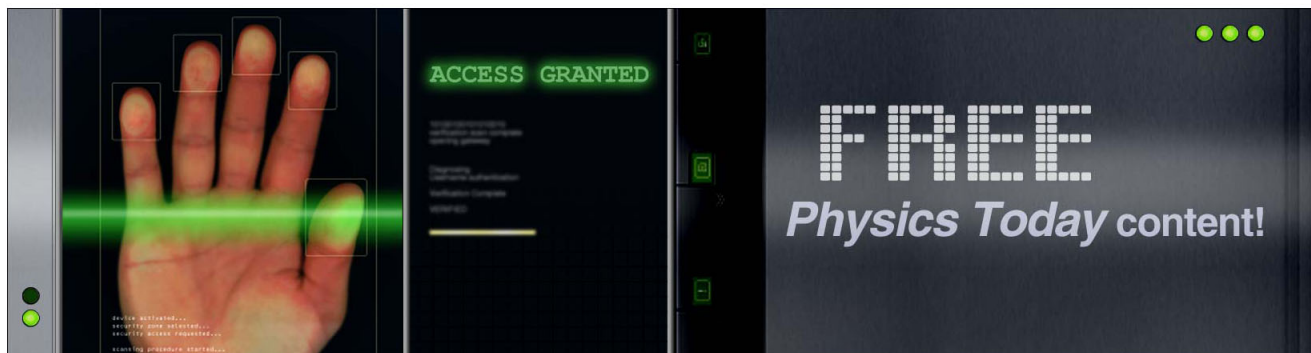
Journal Homepage: <http://apl.aip.org/>

Journal Information: http://apl.aip.org/about/about_the_journal

Top downloads: http://apl.aip.org/features/most_downloaded

Information for Authors: <http://apl.aip.org/authors>

ADVERTISEMENT



Enhanced mobility of organic thin film transistors by water absorption of collagen hydrolysate gate dielectric

Chao-Ying Hsieh,¹ Jenn-Chang Hwang,^{1,a)} Ting-Hao Chang,¹ Jiun-Yi Li,¹ Shih-Han Chen,¹ Lung-Kai Mao,¹ Li-Shiuan Tsai,¹ Yu-Lun Chueh,¹ Ping-Chiang Lyu,² and Shawn S. H. Hsu³

¹Department of Materials Science and Engineering, National Tsing Hua University, Hsin-Chu City 30043, Taiwan

²Department of Life Science, National Tsing Hua University, Hsin-Chu City 30043, Taiwan

³Department of Electrical Engineering, National Tsing Hua University, Hsin-Chu City 30013, Taiwan

(Received 17 April 2013; accepted 16 June 2013; published online 11 July 2013)

Collagen hydrolysate is a nature protein, which works well as the gate dielectric for organic thin film transistors (OTFTs). The pentacene OTFTs exhibit a field-effect mobility (μ_{FE}) value of $0.8 \text{ cm}^2 \text{ V}^{-1} \text{ s}^{-1}$ and an on/off ratio of 10^5 in vacuum. The drain current is greatly enhanced and the μ_{FE} value increases to ca. $15.5 \text{ cm}^2 \text{ V}^{-1} \text{ s}^{-1}$ when OTFTs are exposed to air. The enhancement of μ_{FE} is attributed to the interaction of water and OH-groups in collagen hydrolysate in air ambient.

© 2013 AIP Publishing LLC. [<http://dx.doi.org/10.1063/1.4813075>]

Organic thin film transistors (OTFTs) have great potential in a wide range of applications such as flexible electronics,^{1,2} radio frequency identification (RFID) tags,^{3,4} and sensors.^{5,6} The field-effect mobility (μ_{FE}) of OTFTs is mainly affected by the organic material in the active layer. The dielectric material is another factor able to influence the μ_{FE} value of OTFTs. Inorganic materials (e.g., SiO_2 , Al_2O_3)^{7,8} and polymer (e.g., polyvinyl alcohol (PVA), poly(methyl methacrylate) (PMMA), poly(4-vinylphenol) (PVP))^{9–11} are frequently utilized as the gate dielectrics for OTFTs. Recently, bio-materials have become attractive candidates as the gate dielectrics because of low cost, insulating, and biodegradability. Bio-materials such as DNA-hexadecyltrimethylammonium chloride (DNA-CTMA),¹² lactose and glucose¹³ have been demonstrated as the gate dielectrics for OTFTs. The reported μ_{FE} value ranges from 0.05 to $0.1 \text{ cm}^2 \text{ V}^{-1} \text{ s}^{-1}$. In 2011, silk fibroin was reported to be an excellent gate dielectric for pentacene OTFTs with an average μ_{FE} value as high as ca. $22 \text{ cm}^2 \text{ V}^{-1} \text{ s}^{-1}$.¹⁴ The discovery of silk fibroin has stimulated the search of other natural proteins to be the gate dielectrics for OTFTs. A natural protein is usually composed of its unique sequence of amino residues. The major amino residues of silk fibroin are glycine and alanine that are expected different from other natural proteins. In order to deeper understand the role of protein as the gate dielectric, it is important to accumulate more experimental data of natural proteins as the gate dielectrics.

Practical criterions of natural proteins for OTFTs are low-cost and market availability. In this article, we report the discovery of collagen hydrolysate as the gate dielectric for pentacene OTFTs with good device characteristics in vacuum and in air ambient. Collagen is a protein mainly present in the connective tissues of mammalian. The repeated amino acid sequence of collagen has been reported to be Gly-X-Y, where Gly is the glycine, X is the frequently proline, and Y is the frequently hydroxyproline.^{15,16} Gly-Pro-Hyp is the

most stable sequence of amino acid residues in collagen. The triple helix structure of collagen is stabilized by the hydrogen bonding between carbonyl groups and hydroxyl (-OH) groups of hydroxyproline. Collagen hydrolysate is a hydrolyzed product of collagen,^{17,18} which has been widely used as food additives and cosmetics owing to low-cost, good biocompatibility, and water solubility. The compositions and the repeated sequence of amino acid residues in collagen hydrolysate is similar to that of collagen.¹⁸ The fabrication of the collagen hydrolysate dielectric layer is an aqueous solution process, which is simple and easy to be implemented in the fabrication process of OTFTs.

An array of pentacene OTFT devices and metal-insulator-metal (MIM) structures were fabricated on the polyethylene terephthalate (PET) substrate. The configuration of a pentacene OTFT with collagen hydrolysate as the gate dielectric and the Au/collagen hydrolysate/Ag MIM structure is schematically shown in Fig. 1(a). A 70 nm-thick Ag was thermally evaporated onto PET to define the gate electrode through a shadow mask. The fabrication of the collagen hydrolysate thin film is an aqueous solution process. A powder of collagen hydrolysate (Nitta), a food-grade additive extracted from fish, was dissolved in de-ionized water to obtain a 4 wt. % aqueous solution. The secondary structure of collagen hydrolysate in the aqueous solution is random coil supported by the circular dichroism (CD) spectrum in Fig. 1(b). This indicates that the triple helix structure of collagen is denatured into random coil after hydrolysis, consistent with previously published results.¹⁹ A collagen hydrolysate thin film was coated on PET patterned with Ag gate electrodes by spin coating using the aqueous solution. A dipping process may be required in order to obtain a thicker collagen hydrolysate thin film. The coated collagen hydrolysate thin film was finally cast at 50°C in air. The film thickness of collagen hydrolysate is determined to be ca. 350 nm by field-emission scanning electron microscope (FESEM). The collagen hydrolysate thin film was determined to be amorphous based on the X-ray diffraction data. The root mean square (RMS) roughness of the collagen hydrolysate

^{a)} Author to whom correspondence should be addressed. Electronic mail: jch@mx.nthu.edu.tw

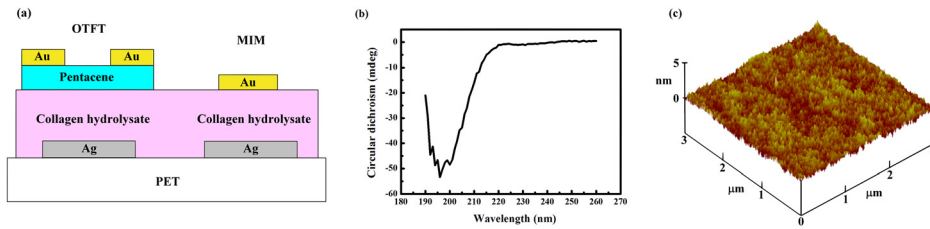


FIG. 1. (a) Schematic showing the pentacene OTFT with collagen hydrolysate as the gate dielectric. (b) Circular dichroism spectrum of collagen hydrolysate. (c) AFM image of the collagen hydrolysate thin film.

thin film is ca. 0.26 nm based on the AFM image in Fig. 1(c). A 65 nm pentacene (99%, Sigma-Aldrich) layer was then deposited on the collagen hydrolysate thin film at a rate of 0.3 \AA/s by thermal evaporation at room temperature. The crystal quality of pentacene on collagen hydrolysate was characterized by grazing-angle incidence X-ray diffraction (GIXD). Au was used to define the source and drain electrodes by thermal evaporation through a shadow mask. The channel length is $50 \text{ }\mu\text{m}$ and the channel width is $600 \text{ }\mu\text{m}$ for each OTFT device. The output characteristics and transfer curves of OTFTs were taken in air ambient using the Agilent 4155C semiconductor parameter analyzer and in vacuum (ca. 5×10^{-2} Torr) using Agilent B1500A semiconductor device analyzer. The humidity in air ambient ranges from 60% to 70% in the I-V tests.

The MIM structure with ca. 350 nm collagen hydrolysate as the insulator was fabricated next to each OTFT in order to measure the accurate capacitance value for the derivation of μ_{FE} . The dimensions of MIM structures are $400 \text{ }\mu\text{m}$ in width and $600 \text{ }\mu\text{m}$ in length. The quasi-static capacitance-voltage method was used to measure the capacitance of the MIM structure using Agilent B1500A. The voltage across the MIM structure was swept step by step from the “start” to the “stop” voltage. A sweep rate of 0.08 V/s was used to simulate the transfer curve operation. At each sweep step, current (I) and voltage were measured during the voltage transition (ΔV). Capacitance was calculated in Agilent B1500A by using the equation $C = \Delta Q/\Delta V$, where ΔQ is the net charge integrated over the integration time.

Fig. 2(a) shows the typical output characteristics of a pentacene OTFT taken in vacuum, with collagen hydrolysate as the gate dielectric. The transfer characteristics in Fig. 2(b) show a low leakage current of $3 \times 10^{-11} \text{ A}$, a subthreshold swing of 1.6 V/decade and an on/off ratio of 2×10^5 . The threshold voltage (V_{TH}) and the field-effect mobility in the saturation regime ($\mu_{\text{FE,sat}}$) can be derived from the $I_{\text{D}}^{1/2}$ versus V_{G} curve shown in the inset in Fig. 2(b). The $\mu_{\text{FE,sat}}$ value is obtained from the relationship

$$I_{\text{D}} = (C_i \mu_{\text{FE,sat}} W/2L)(V_{\text{G}} - V_{\text{TH}})^2,$$

where W is the channel width, L is the channel length, C_i is the capacitance per unit area of the gate dielectric, V_{G} is the gate voltage, and V_{TH} is the threshold voltage. The C_i value in vacuum was measured to be 8 nF/cm^2 as shown in the quasi-static capacitance (QSC) versus voltage curve [Fig. 2(c)]. And the $\mu_{\text{FE,sat}}$ value and V_{TH} are determined to be $0.8 \text{ cm}^2 \text{ V}^{-1} \text{ s}^{-1}$ and -12 V , respectively. The maximum interface trap density (N_{SS}) is estimated to be $1.2 \times 10^{12} \text{ cm}^{-2} \text{ eV}^{-1}$ using the equation²⁰

$$N_{\text{SS}} = \left[\frac{S \cdot \log(e)}{kT/q} - 1 \right] \cdot \frac{C_i}{q},$$

where S is the subthreshold swing, k is the Boltzmann’s constant, T is the absolute temperature, and C_i is the capacitance per unit area.

A peculiar phenomenon is the enhancement of drain current when OTFTs are exposed to air from vacuum. Fig. 3(a) shows the square root plot of the transfer characteristics of an OTFT device vented to air after 0, 5, 10, and 20 min. The drain current rapidly increases with time from ca. 10^{-9} to 10^{-5} A at $V_{\text{G}} = -3 \text{ V}$ and saturates at ca. 10^{-5} A after 20 min air exposure as illustrated in Fig. 3(b). The V_{TH} value also reduces with air exposure time and down to -0.5 V after 20 min air exposure.

The device characteristics of OTFTs in air ambient are quite different from those in vacuum. Fig. 3(c) shows the output characteristics of a typical pentacene OTFT in air ambient. A saturation current of ca. $17 \text{ }\mu\text{A}$ is achieved at a drain voltage (V_{D}) of -7 V , while V_{G} is set at -3 V . A small protrusion appears at $V_{\text{D}} = \text{ca. } -6 \text{ V}$ in Fig. 3(c), which was also observed in the output characteristics of pentacene OTFTs in air ambient with DNA-CTMA¹² or silk fibroin¹⁴ as the gate dielectric. Note that the output characteristics are nonlinear at very low V_{D} . The drain voltage deviated from the linearity, i.e., ΔV shown in Fig. 3(c), is attributed to the

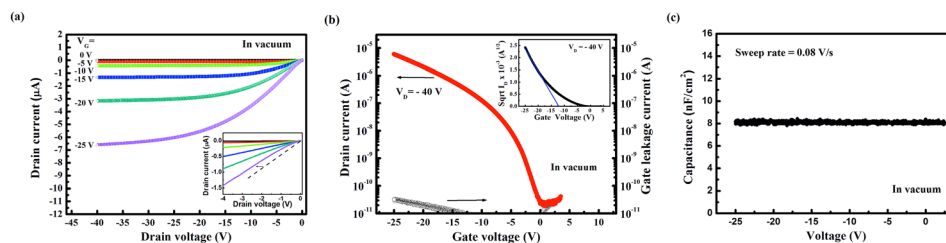


FIG. 2. Electrical characteristics of a pentacene OTFT with collagen hydrolysate as the gate dielectric and an Au/collagen hydrolysate/Ag MIM structure. The measurements were taken in vacuum (ca. 5×10^{-2} Torr). (a) Output characteristics. The inset is the enlarged output curves at low V_{D} . (b) Transfer and gate leakage current characteristics. The inset is the $I_{\text{D}}^{1/2}$ versus V_{G} plot for the determination of $\mu_{\text{FE,sat}}$. (c) Quasi-static capacitance versus voltage curve of the MIM structure taken at a sweep rate of 0.08 V/s .

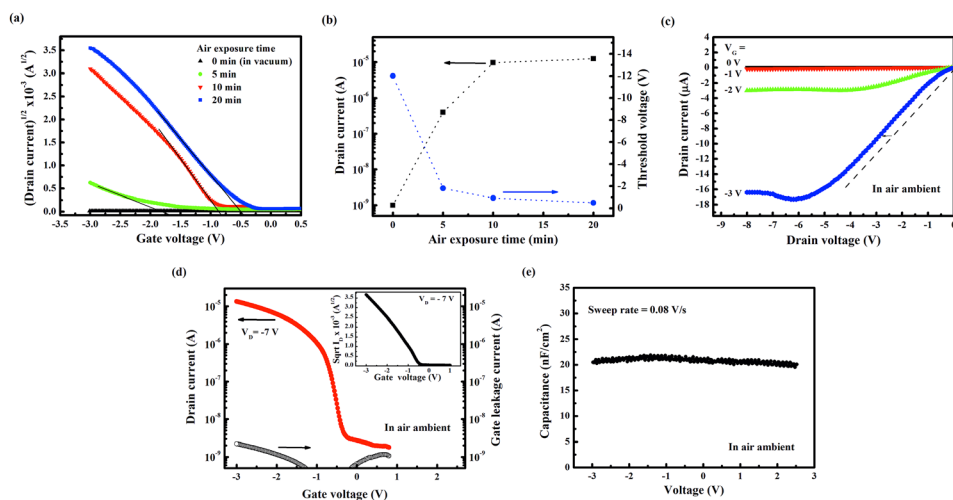


FIG. 3. Electrical characteristics of a pentacene OTFT with collagen hydrolysate as gate dielectric, taken after exposing the device to air ambient from vacuum. (a) $I_D^{1/2}$ versus V_G plot after 0, 5, 10, and 20 min air exposure. (b) Drain current and threshold voltage as a function of air exposure time. (c) Output characteristics. (d) Transfer and gate leakage current characteristics taken after 30 min air exposure. The inset is the $I_D^{1/2}$ versus V_G plot for the determination of $\mu_{FE,sat}$. (e) Quasi-static capacitance versus voltage curve of the MIM structure taken at a sweep rate of 0.08 V/s.

existence of a Schottky barrier height between the electrodes and the active layer, similar to what has been proposed in the literature.^{21,22} The Schottky barrier height may be resulted from the formation of the interface dipole between pentacene and the electrode Au, which was supported by the X-ray and Ultra-violet photoemission data.²³ The hole injection barrier at the Au/pentacene interface can be as large as 1 eV, resulting in the increase of the contact resistance. If the existence of Schottky barrier is correct, the nonlinear character at very low V_D should be also found in the output characteristics in vacuum [Fig. 2(a)]. The non-linearity indeed appears in vacuum when the output curves at low V_D is enlarged, as shown in the inset in Fig. 2(a). This supports the existence of the Schottky barrier induced contact resistance for the pentacene OTFTs in air ambient and in vacuum. Note that I_D will be further increased if the Schottky barrier induced contact resistance does not exist.

The transfer characteristics in air ambient exhibits and a gate leakage current less than 2×10^{-9} A, an on/off current ratio of 5×10^3 and a low a subthreshold swing of 0.19 V/decade as shown in Fig. 3(d). The QSC value of the MIM structure in air was measured to be 22 nF/cm² [Fig. 3(e)] that is higher than that in vacuum. The $\mu_{FE,sat}$ value and V_{TH} of the OTFT device are determined to be $16 \text{ cm}^2\text{V}^{-1}\text{s}^{-1}$ and -0.4 V, respectively. The average $\mu_{FE,sat}$ value is $15.5 \pm 1.7 \text{ cm}^2\text{V}^{-1}\text{s}^{-1}$ based on 10 test devices. The derived N_{SS} value is ca. $3.1 \times 10^{11} \text{ cm}^{-2} \text{ eV}^{-1}$, which is much less than that for the OTFTs in vacuum.

The device performance of the pentacene OTFT in air ambient is much better than that in vacuum. In general, a high μ_{FE} value of a pentacene OTFT may be contributed from structure factors such as good crystal quality of pentacene (e.g., large grain size) and low interface trap density and small surface roughness of the gate dielectric. The crystal quality of pentacene was characterized by GIXD, the amount of the thin film phase pentacene on collagen hydrolysate is ca. three times larger than that on SiO₂, supported by their relative peak intensity at $2\theta = 5.7^\circ$ in Fig. 4. The better pentacene crystal quality may explain our $\mu_{FE,sat}$ value of $0.8 \text{ cm}^2\text{V}^{-1}\text{s}^{-1}$ slightly larger than $0.22 \text{ cm}^2\text{V}^{-1}\text{s}^{-1}$ for the OTFT with SiO₂ as the gate dielectric.¹⁴

Note that the crystal quality of pentacene and the surface roughness of collagen hydrolysate are the same for each

pentacene OTFT in air ambient and in vacuum. The high $\mu_{FE,sat}$ value of the pentacene OTFT in air ambient is attributed to the interaction between water and the OH-groups in collagen hydrolysate. The OH-groups can be found in the hydroxyproline amino acid residues in collagen hydrolysate. Lee *et al.*²⁴ reported that the μ_{FE} value in air increases with the number of the OH-group in polymeric dielectric. The I_D value also increases by approximately two orders of magnitude. Similarly in our case, the $\mu_{FE,sat}$ value increases from 0.8 to $15.5 \text{ cm}^2\text{V}^{-1}\text{s}^{-1}$ and I_D increases from ca. 10^{-9} to 10^{-5} A at $V_G = -3$ V when the OTFT is exposed to air. Recently, Zan and Hsu further proposed that negatively charged O^- groups and H_3O^+ ions was generated in PVP in air ambient, which help to accumulate holes and to result in higher μ_{FE} .²⁵ Similarly, negatively charged O^- groups and H_3O^+ ions are proposed to be generated in collagen hydrolysate by the reaction below.

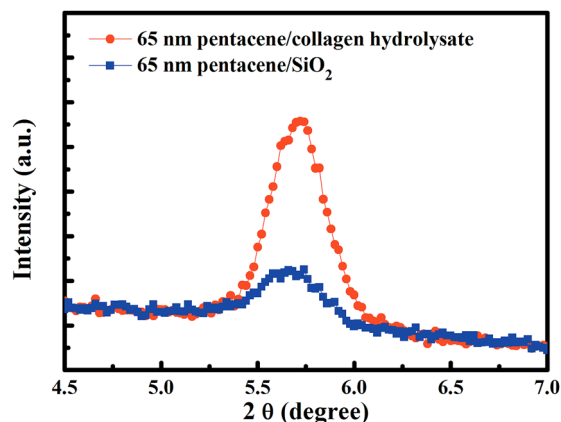
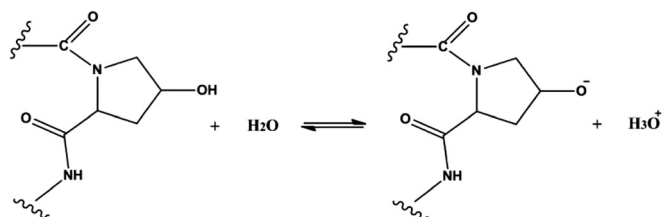


FIG. 4. GIXRD spectra of 65 nm pentacene deposited on collagen hydrolysate and SiO₂.

The hydroxyproline amino residue with O^- group in collagen hydrolysate is immobile because of its large size. In contrast, H_3O^+ ions are mobile which would migrate toward the gate electrode when the gate electrode is negatively biased. The QSC value of collagen hydrolysate would increase due to the movement of H_3O^+ ions. The reduction of V_{TH} from -12 to -0.4 V after air exposure can be partially explained by the increase of the QSC value. Moreover, less hole carriers are needed to fill the trap states before turn-on due to the reduction of the N_{SS} value from 1.2×10^{12} to $3.1 \times 10^{11} \text{ cm}^{-2} \text{ eV}^{-1}$. The low N_{SS} value may have partial contribution to the reduction of V_{TH} . Moreover, the increase of the QSC value also helps to accumulate more holes to fill the interface trap states such that the μ_{FE} value can be enhanced.

In conclusion, collagen hydrolysate works well as the gate dielectric of pentacene OTFTs. The OTFTs exhibit a μ_{FE} value of $0.8 \text{ cm}^2 \text{ V}^{-1} \text{ s}^{-1}$ and an on/off ratio of 10^5 in vacuum. The μ_{FE} value increases to ca. $15.5 \text{ cm}^2 \text{ V}^{-1} \text{ s}^{-1}$ when the OTFTs are exposed to air. The enhancement of μ_{FE} is attributed to the interaction of water and OH-groups in collagen hydrolysate. However, the leakage current increases in air ambient, which causes the reduction of on/off ratio to 5×10^3 . It is important to find a method able to optimize the amount of moisture in the collagen hydrolysate for this kind of OTFT devices.

The authors like to thank the financial support from National Science Council, Republic of China through the project NSC 100-2221-E-007-067-MY3.

¹G. H. Gelinck, H. E. A. Huitema, E. van Veenendaal, E. Cantatore, L. Schrijnemakers, J. B. P. H. van der Putten, T. C. T. Geuns, M. Beenhakkers, J. B. Giesbers, B.-H. Huisman, E. J. Meijer, E. M. Benito, F. J. Touwslager, A. W. Marsman, B. J. E. van Rens, and D. M. de Leeuw, *Nat. Mater.* **3**, 106 (2004).

- ²T. Sekitani, U. Zschieschang, H. Klauk, and T. Someya, *Nat. Mater.* **9**, 1015 (2010).
- ³E. Cantatore, T. C. T. Geuns, G. H. Gelinck, E. van Veenendaal, A. F. A. Gruijthuisen, L. Schrijnemakers, S. Drews, and D. M. de Leeuw, *IEEE J. Solid-State Circuits* **42**, 84 (2007).
- ⁴K. Myny, S. Steudel, S. Smout, P. Vicca, F. Furthner, B. van der Putten, A. K. Tripathi, G. H. Gelinck, J. Genoe, W. Dehaene, and P. Heremans, *Org. Electron.* **11**, 1176 (2010).
- ⁵H. U. Khan, M. E. Roberts, O. Johnson, R. Förch, W. Knoll, and Z. Bao, *Adv. Mater.* **22**, 4452 (2010).
- ⁶H. U. Khan, M. E. Roberts, W. Knoll, and Z. Bao, *Chem. Mater.* **23**, 1946 (2011).
- ⁷K. D. Kim and C. K. Song, *Appl. Phys. Lett.* **88**, 233508 (2006).
- ⁸H. Klauk, D. J. Gundlach, J. A. Nichols, and T. N. Jackson, *IEEE Trans. Electron Devices* **46**, 1258 (1999).
- ⁹Y. Jang, D. H. Kim, Y. D. Park, J. H. Cho, M. Hwang, and K. Cho, *Appl. Phys. Lett.* **88**, 072101 (2006).
- ¹⁰C. Kim, A. Facchetti, and T. J. Marks, *Science* **318**, 76 (2007).
- ¹¹J. Puigdollers, C. Voz, A. Orpella, R. Quidant, I. Martín, M. Vetter, and R. Alcubilla, *Org. Electron.* **5**, 67 (2004).
- ¹²B. Singh, N. S. Sariciftci, J. G. Grote, and F. K. Hopkins, *J. Appl. Phys.* **100**, 024514 (2006).
- ¹³M. Irimia-Vladu, P. A. Troshin, M. Reisinger, G. Schwabegger, M. Ullah, R. Schwoedlauer, A. Mumyatov, M. Bodea, J. W. Ferguson, V. F. Razumov, H. Sitter, S. Bauer, and N. S. Sariciftci, *Org. Electron.* **11**, 1974 (2010).
- ¹⁴C.-H. Wang, C.-Y. Hsieh, and J.-C. Hwang, *Adv. Mater.* **23**, 1630 (2011).
- ¹⁵A. Rich and F. H. C. Crick, *Nature* **176**, 915 (1955).
- ¹⁶S. K. Holmgren, K. M. Taylor, L. E. Bretscher, and R. T. Raines, *Nature* **392**, 666 (1998).
- ¹⁷B. Li, F. Chen, X. Wang, B. Ji, and Y. Wu, *Food Chem.* **102**, 1135 (2007).
- ¹⁸Y. Zhuang, H. Hou, X. Zhao, Z. Zhang, and B. Li, *J. Food Sci.* **74**, H183 (2009).
- ¹⁹Z. K. Zhang, G. Y. Li, and B. Shi, *J. Soc. Leather Technol. Chem.* **90**, 23 (2006).
- ²⁰K. N. N. Unni, S. Dabos-Seignon, and J. M. Nunzi, *J. Phys. D: Appl. Phys.* **38**, 1148 (2005).
- ²¹B. H. Hamadani and D. Natelson, *J. Appl. Phys.* **97**, 064508 (2005).
- ²²D. J. Gundlach, L. Zhou, J. A. Nichols, and T. N. Jackson, *J. Appl. Phys.* **100**, 024509 (2006).
- ²³N. J. Watkins, L. Yan, and Y. Gao, *Appl. Phys. Lett.* **80**, 4384 (2002).
- ²⁴S. Lee, B. Koo, J. Shin, E. Lee, and H. Park, *Appl. Phys. Lett.* **88**, 162109 (2006).
- ²⁵H.-W. Zan and T.-Y. Hsu, *IEEE Electron Device Lett.* **32**, 1131 (2011).